



**Serbian Ceramic Society Conference
ADVANCED CERAMICS AND APPLICATION IV**

**Serbian Academy of Sciences and Arts, Knez Mihailova 35
Serbia, Belgrade,
21-23. September 2015**

THERMAL TREATMENT OF OXIDES IN DIFFERENT ATMOSPHERES

**Nebojša Labus¹, Zorka Z. Vasiljević¹,
Slavko Mentus^{2,3}, Vladimir B. Pavlović¹,
Miloljub Luković⁴, Maria Vesna Nikolić⁴**

¹Institute of Technical Sciences of SASA, Knez 35, 11000
Belgrade, Serbia

²Faculty of Physical Chemistry, Studentski trg 12-16, 11158
Belgrade, University of
Belgrade, Serbia

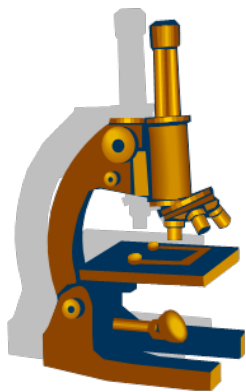
³Serbian Academy of Sciences and Arts, Knez Mihailova 35,
11000 Belgrade, Serbia

⁴Institute for Multidisciplinary Research, Kneza Višeslava 1,
11000 Belgrade, University of Belgrade, Serbia

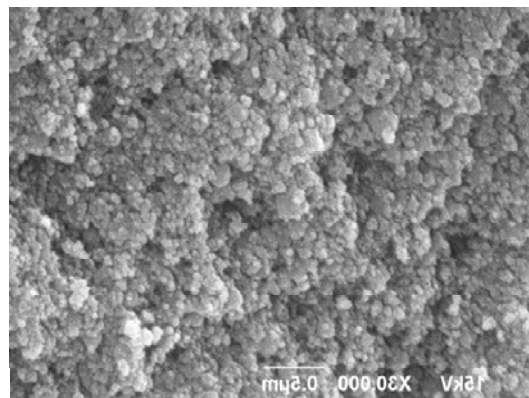
Aim



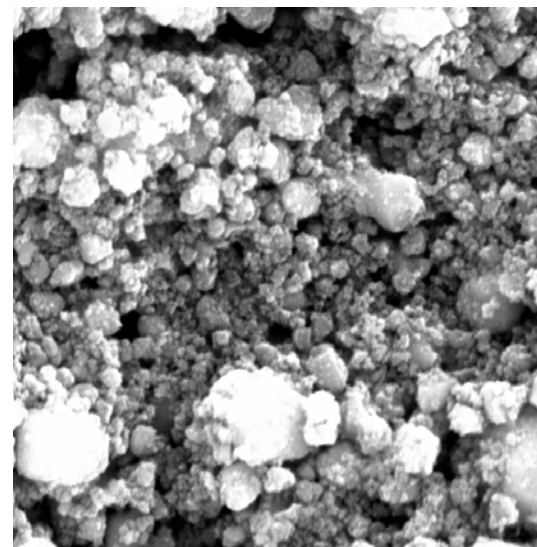
TiO₂ nanopowder,
Alfa Aesar 99.7%
anatase with sizes of
particles from
10 nm to 15 nm



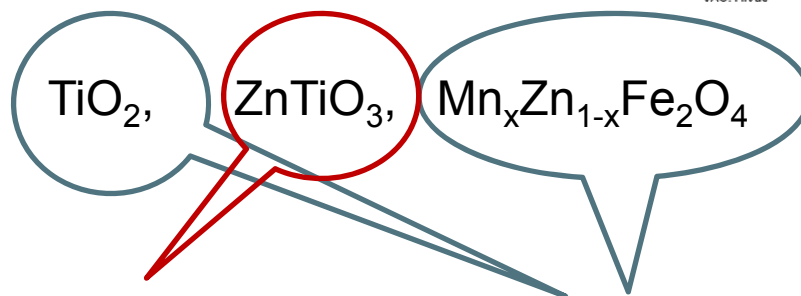
ZnTiO₃ nanopowder,
Aldrich
[CAS 112036-43-0]



Comercial ,
Micro powder
Composition:
Mn_{0.63}Zn_{0.37}Fe₂O₄, 93 wt.%
and Fe₂O₃ 7 wt.%



SEM MAG: 30.00 kx
HV: 20.0 kV
VAC: HiVac
DET: SE Detector
DATE: 03/24/14
Device: VEGA TS 5130MM
2 μm
Vega ©Tescan
Digital Microscopy Imaging



Stoichiometric - nonstoichiometric
compounds

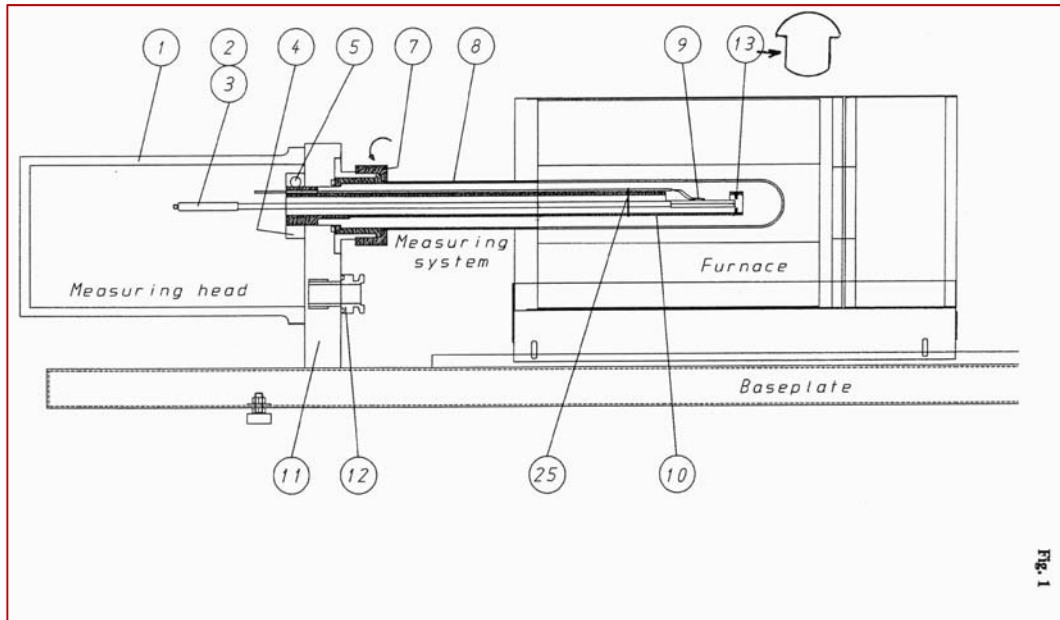
15 nm

30 nm

>1 μm

Technical approach



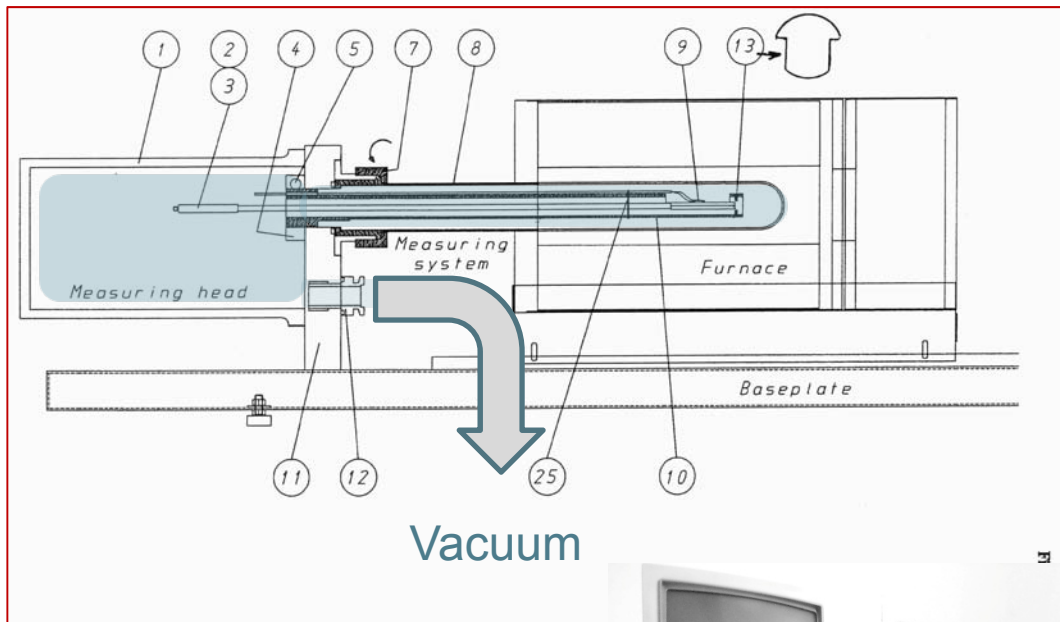


Gas chamber in the dilatometric device and vacuum and atmosphere exits

Vacuum gauge Main pressure valve Manometer Gas inlet and outlet switches
 Flow meter



Atmosphere regulation control unit



Gas chamber in the dilatometric device and vacuum and atmosphere exits

Equipment for the evacuating gas chamber in the dilatometric device



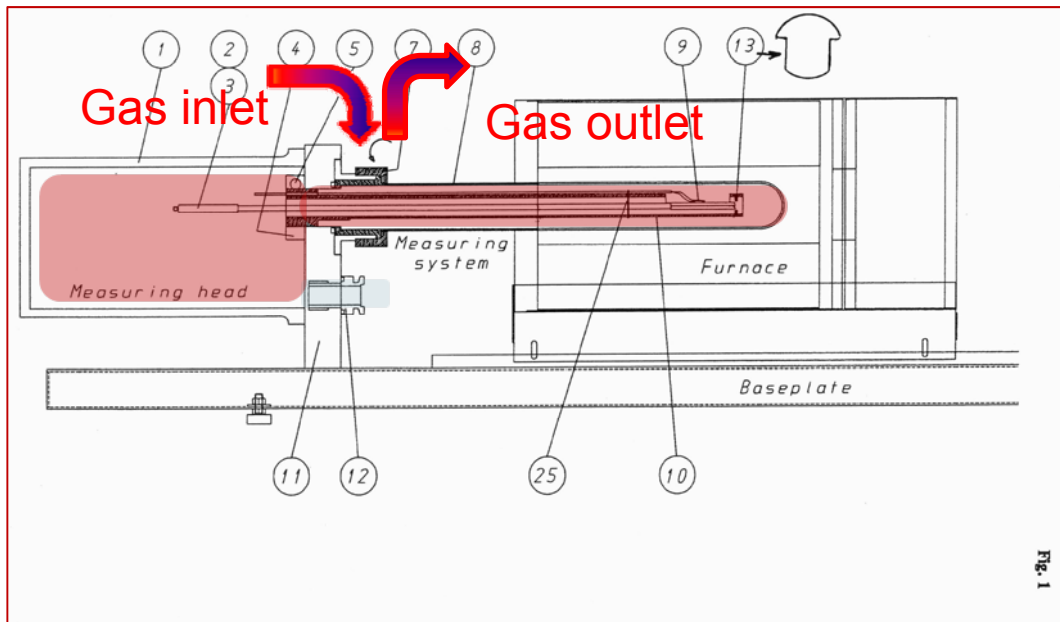


Fig. 1

Gas chamber in the dilatometric device and vacuum and atmosphere exits

Theory - about point defects



POINT DEFECTS AND TRANSPORT IN NON-STOICHIOMETRIC OXIDES:
 SOLVED AND UNSOLVED PROBLEMS

RÜDIGER DIECKMANN

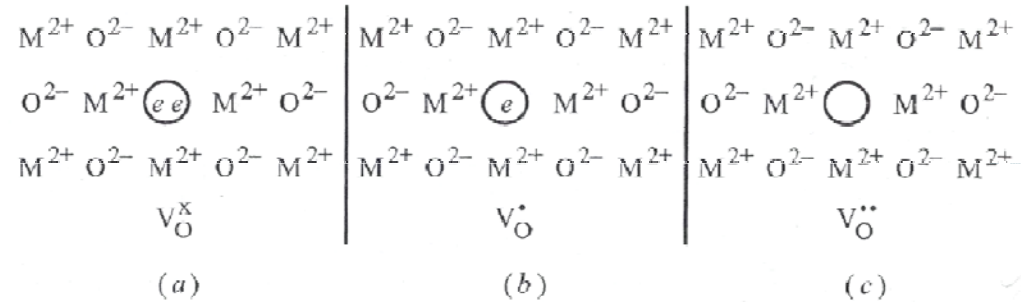


Figure 6.4 (a) The formation of an oxygen vacancy by the loss of an oxygen atom to the gas phase. This is a nonstoichiometric reaction because the crystal chemistry changes as a result. Note that as drawn, the electrons are localized at the vacancy site, rendering its effective charge zero. (b) A V_O^\bullet site is formed when one of these electrons is excited into the conduction band. (c) The escape of the second electron creates a $V_O^{\bullet\bullet}$ site.

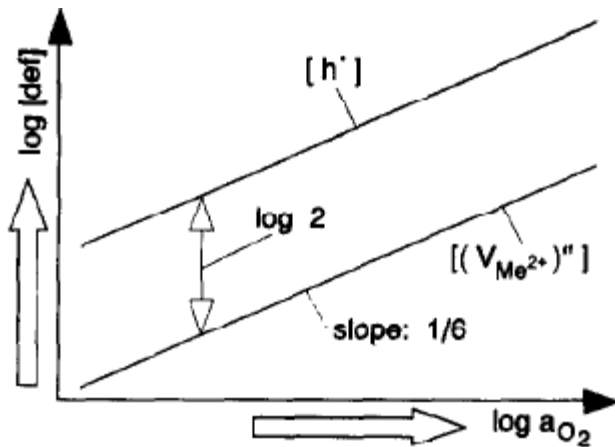
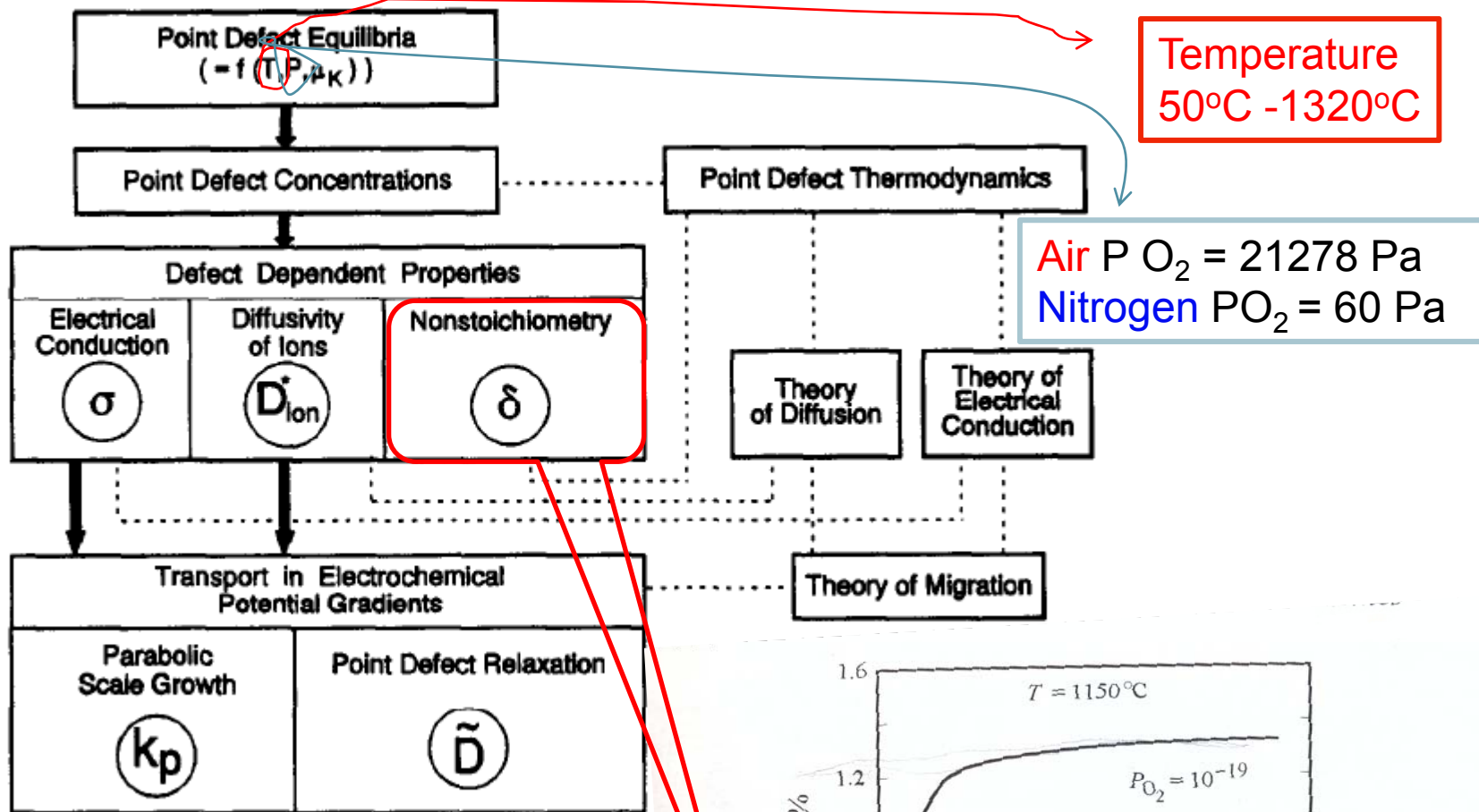
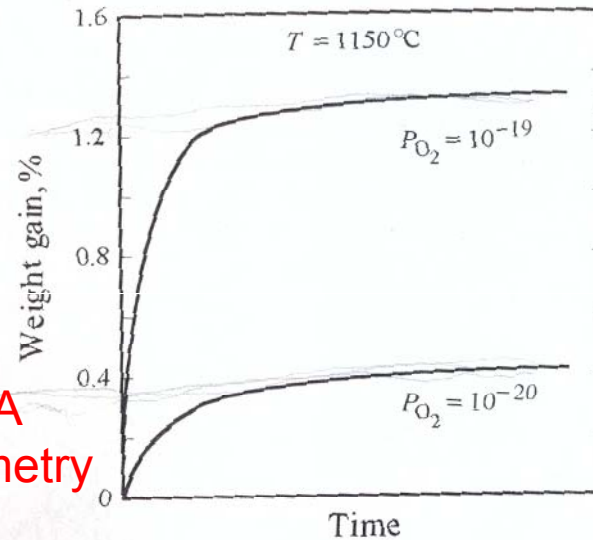


Fig. 3. Schematic plot of the concentrations of cation vacancies, $[(V_{Me^{2+}})^\bullet]$, and of holes, $[h^\bullet]$, in a model oxide of the type $Me_{1-\Delta}O$ with cation vacancies and holes as the majority defects and very small point defect concentrations.



*TG/DTA
*Dilatometry



Typical thermogravimetric results for the oxidation of FeO_x .

TG determination of the non stoichiometry

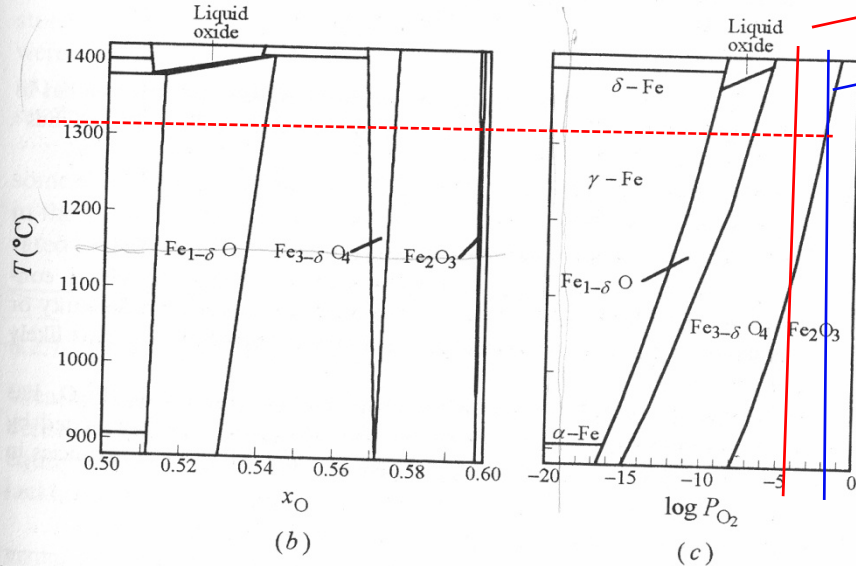


Figure 6.8 (a) Stability domains of various phases in the Mn-O system and the corresponding deviations in stoichiometry.⁷⁸ (b) Phase diagram of Fe-O system, x_O is mole fraction of oxygen, and (c) stability domains of the various phases in Fe-O system.⁷⁹

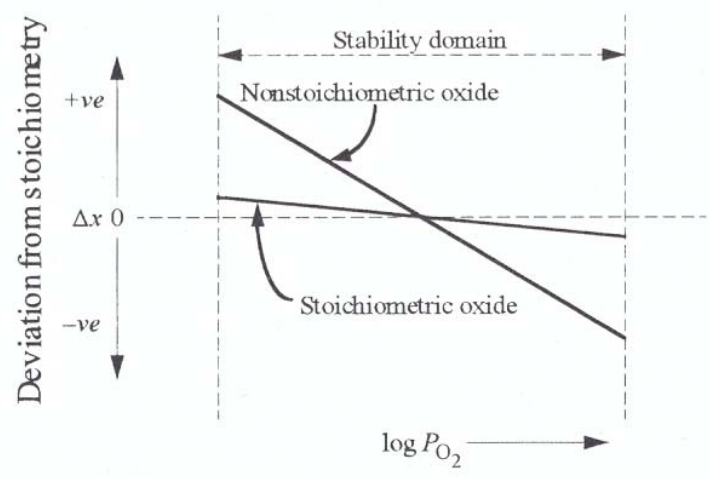
Temperature
50°C - 1320°C

Air $p_{O_2} = 21278 \text{ Pa}$,
 $-\log_{10} p_{O_2} = 4.3279$
 Nitrogen $p_{O_2} = 60 \text{ Pa}$
 $-\log_{10} p_{O_2} = 1.778$

Table 6.1 Range of stoichiometry and existence domains of a number of binary oxides at 1000 K⁷⁷

| Oxides | Deviation from stoichiometry | | | Stability or existence region ¹ - log P _{O₂} | |
|---------------------------------|------------------------------|------------------|-----------------|---|------|
| | x _{min} | x _{max} | Δx ¹ | Min | Max |
| Nonstoichiometric oxides | | | | | |
| TiO | 0.8 | 1.3 | 0.5 | 44.2 [§] | 41.5 |
| Ti ₂ O ₃ | 1.501 | 1.512 | 0.011 | 41.5 | 38.1 |
| TiO ₂ | 1.992 | 2.00 | 0.008 | 25.7 | — |
| V ₂ O ₅ | 0.8 | 1.3 | 0.5 | 35.0 | 33.2 |
| MnO | 1.00 | 1.18 | 0.18 | 34.5 [§] | 10.7 |
| FeO | 1.045 | 1.2 | 0.155 | 21.6 [§] | 17.9 |
| Fe ₃ O ₄ | 1.336 | 1.381 | 0.045 | 17.9 | 10.9 |
| CoO | 1.00 | 1.012 | 0.012 | 17.1 [§] | 2.5 |
| NiO | 1.00 | 1.001 | 0.001 | 16.5 [§] | — |
| Cu ₂ O | 0.500 | 0.5016 | 0.0016 | 9.97 [§] | 7.0 |
| Stoichiometric oxides | | | | | |
| Al ₂ O ₃ | 1.5000 | 1.5000 | — | 71.3 | — |
| MgO | 1.00000 | 1.0000 | — | 51.5 | — |

$x = \frac{b}{a} \pm \delta$ **M_aO_b**
 TiO₂, b/a=2/1=2
 x_{min} = 1.992
 x_{max} = 2.00
 Δx = 0.008
 -log P_{O2}
 Min = 25.07
 Max = /





POINT DEFECTS AND TRANSPORT IN NON-STOICHIOMETRIC OXIDES:
 SOLVED AND UNSOLVED PROBLEMS

RÜDIGER DIECKMANN

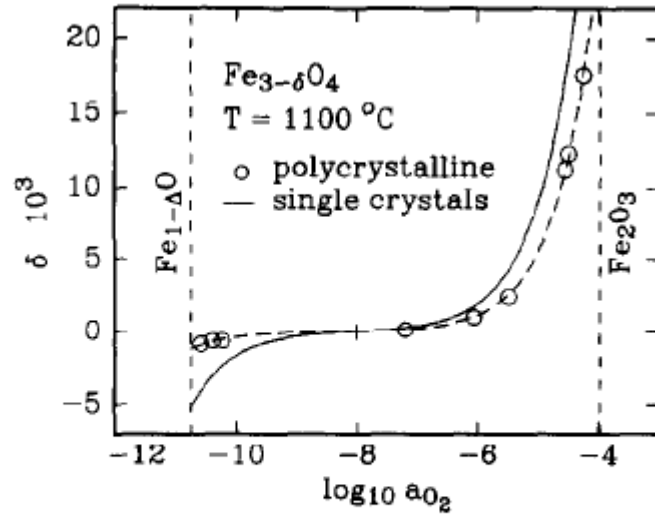


Fig. 19. Variation of δ in single-crystal and polycrystalline $\text{Fe}_{3-\delta}\text{O}_4$ at 1100°C .

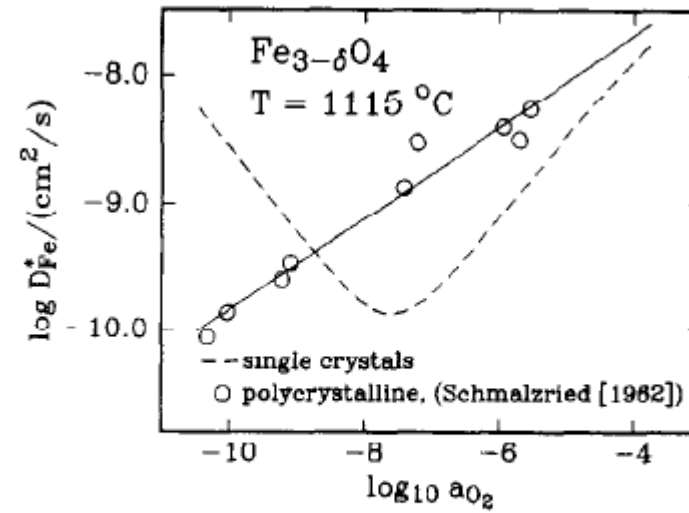


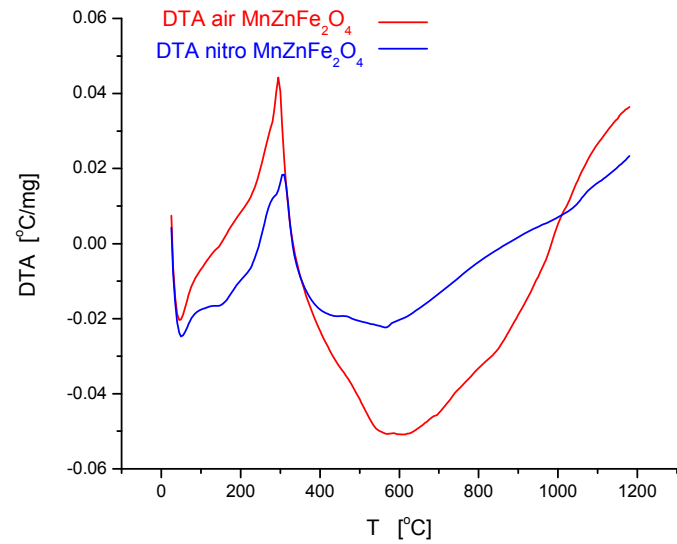
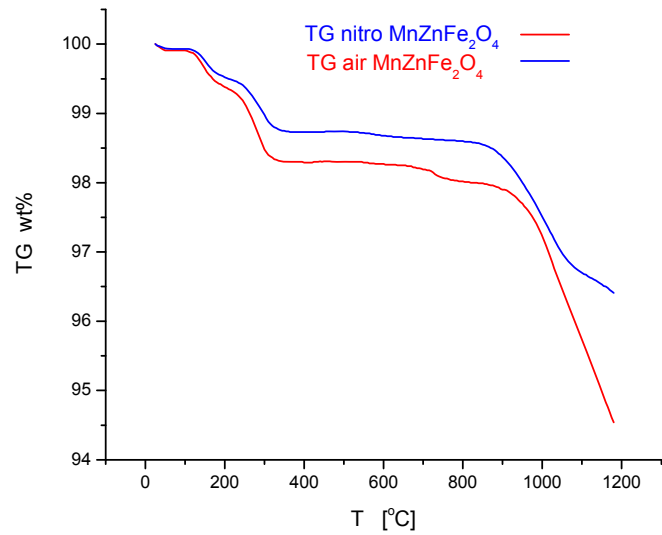
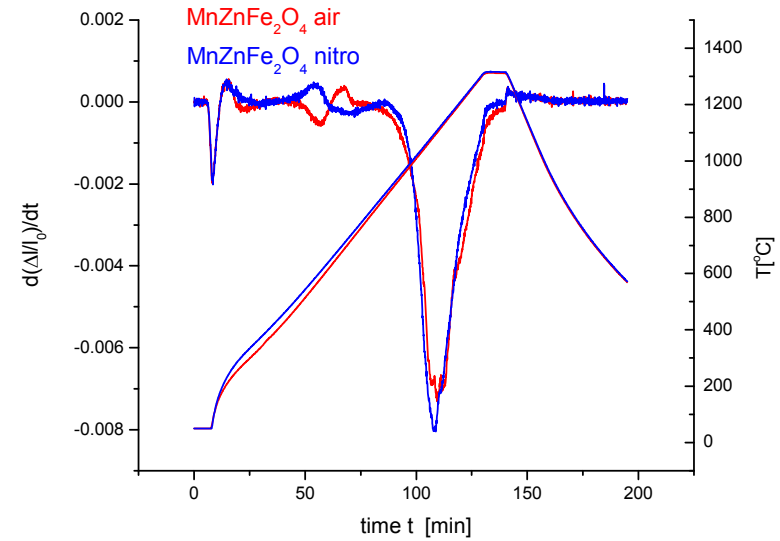
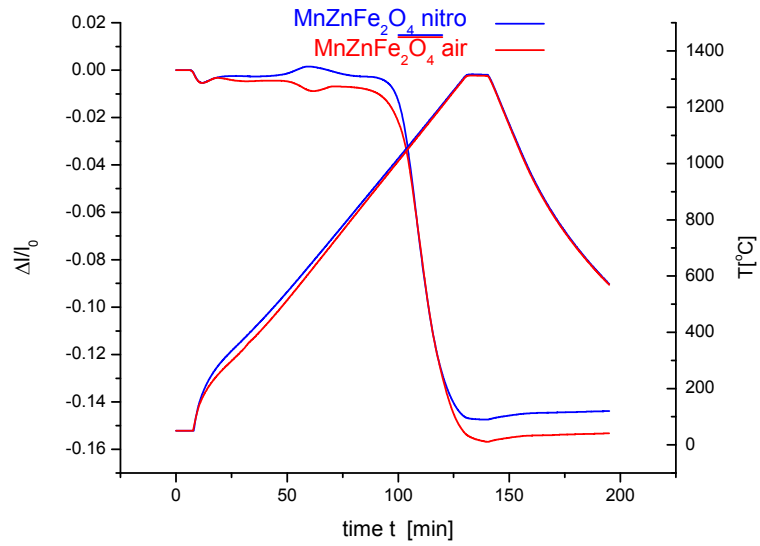
Fig. 20. Oxygen activity dependence of the iron tracer diffusion coefficient, D_{Fe}^* , in single-crystal and polycrystalline $\text{Fe}_{3-\delta}\text{O}_4$ [35] at 1115°C .

Results



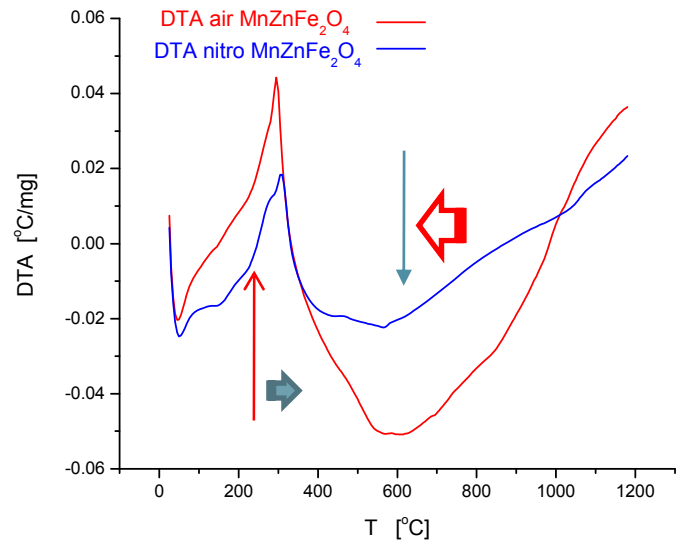
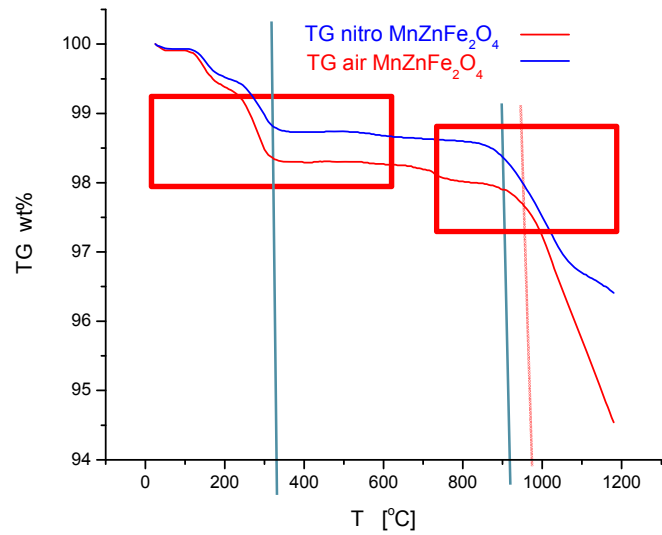
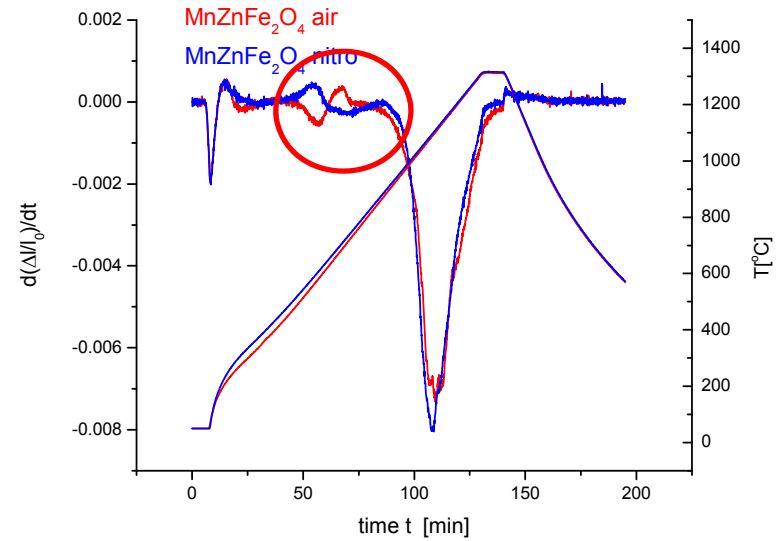
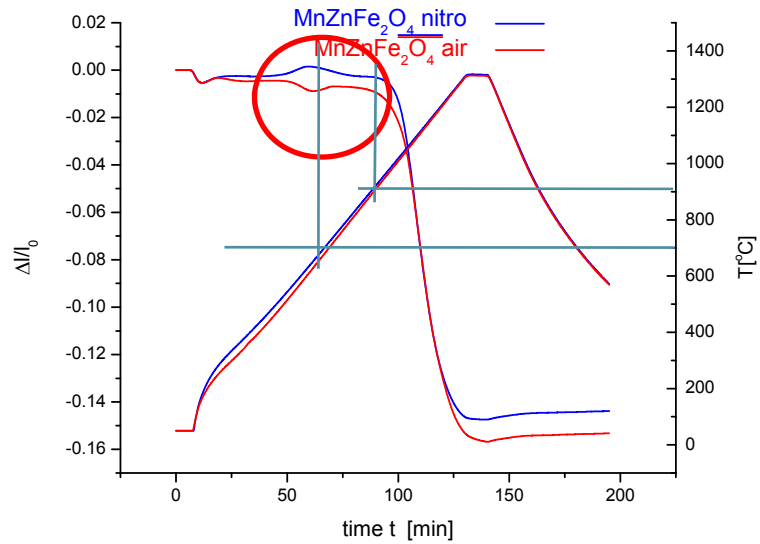
Dilatometry and TG/DTA

$Mn_{1-x}Zn_xFe_2O_4$



Dilatometry and TG/DTA

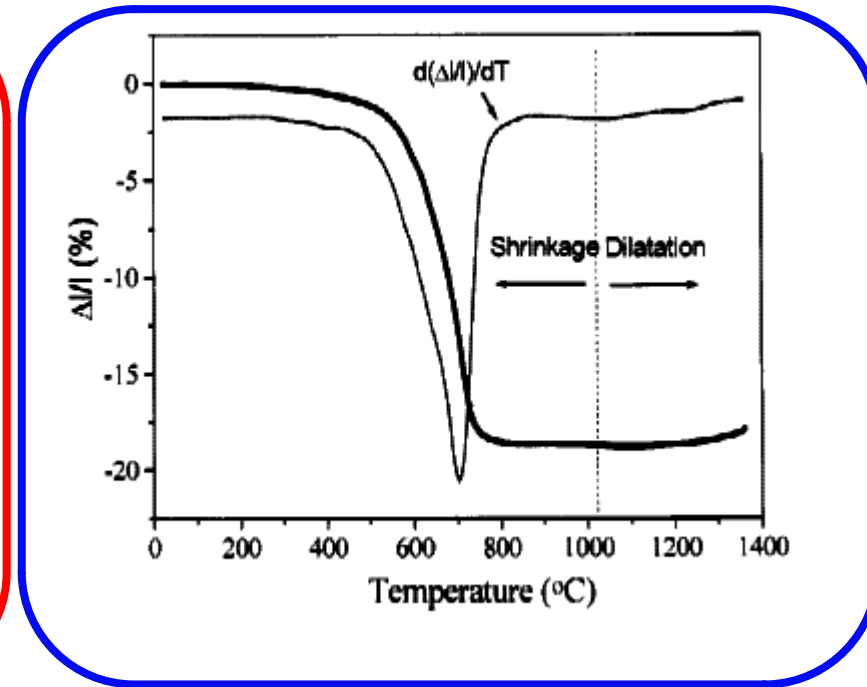
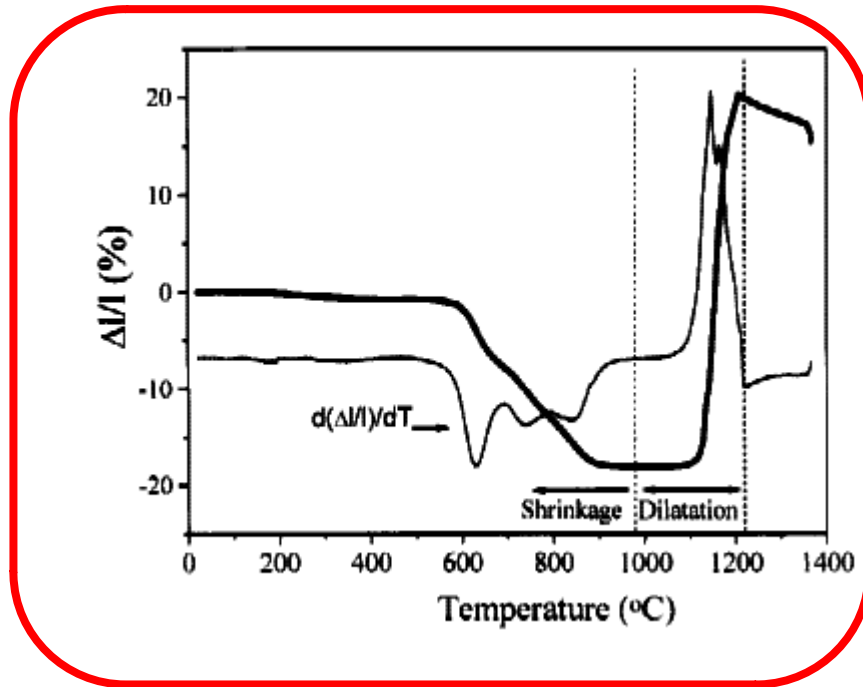
$Mn_{1-x}Zn_xFe_2O_4$





Air

Nitrogen



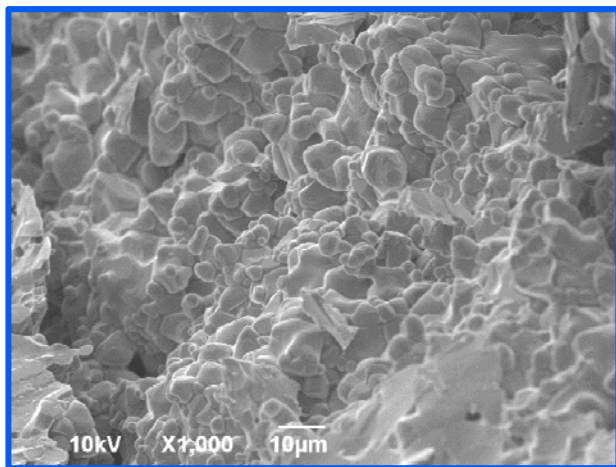
J. Am. Ceram. Soc., 81 [7] 1757-64 (1998)

Sintering of Nanosized MnZn Ferrite Powders

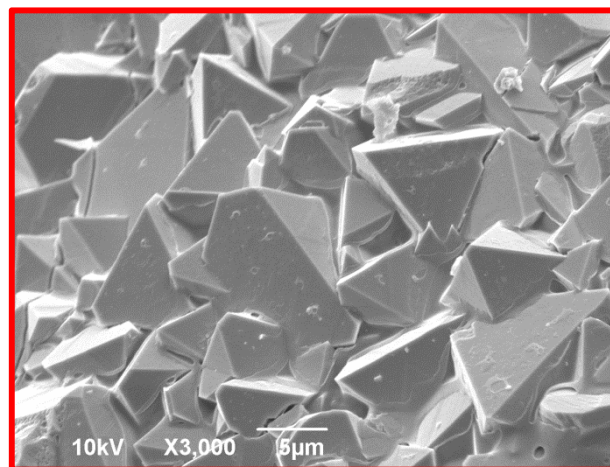
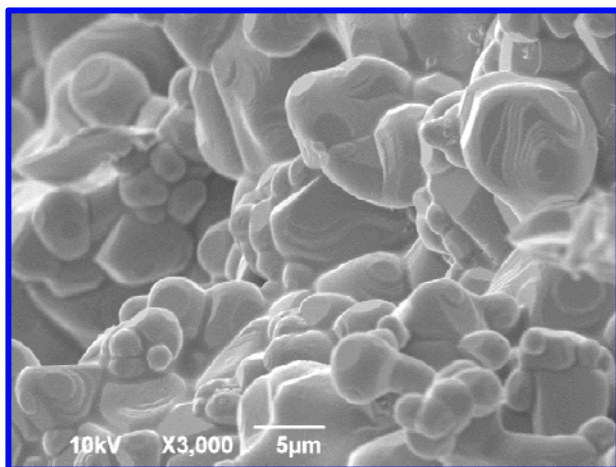
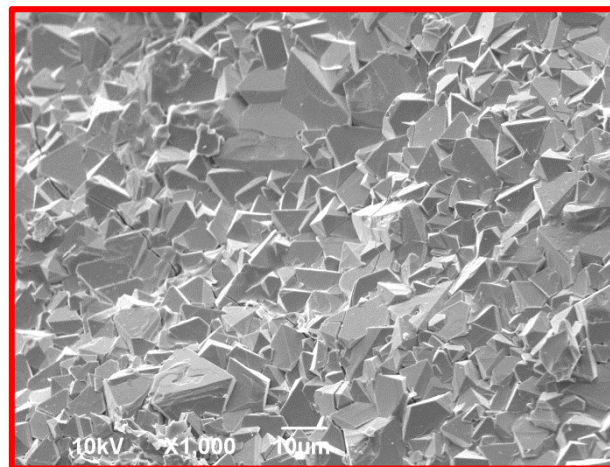
Marko Rozman and Miha Drofenik*
 Jožef Stefan Institute, Ljubljana, Slovenia

SEM $\text{Mn}_{1-x}\text{Zn}_x\text{Fe}_2\text{O}_4$

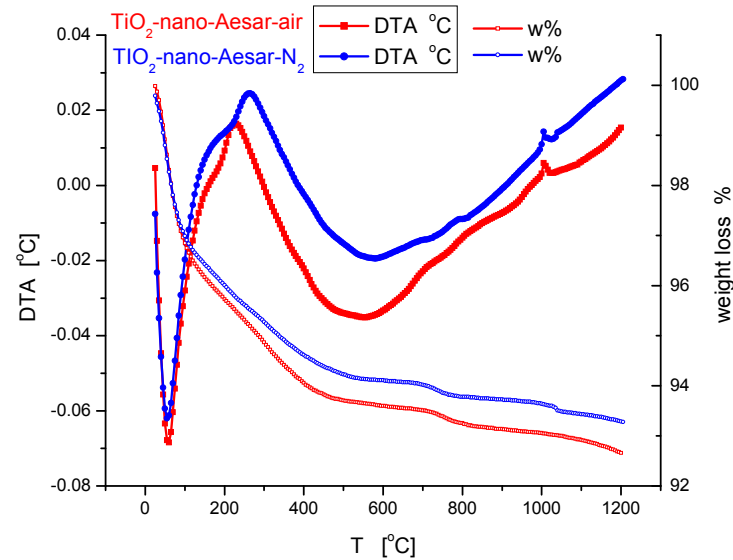
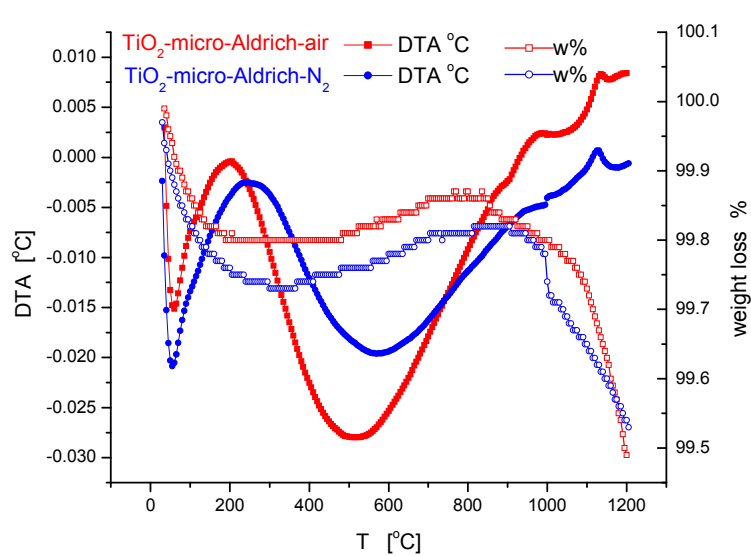
Nitrogen



Air



TiO₂ nano powder TiO₂ micro powder TG/DTA



Science of Sintering, **46** (2014) 365-375

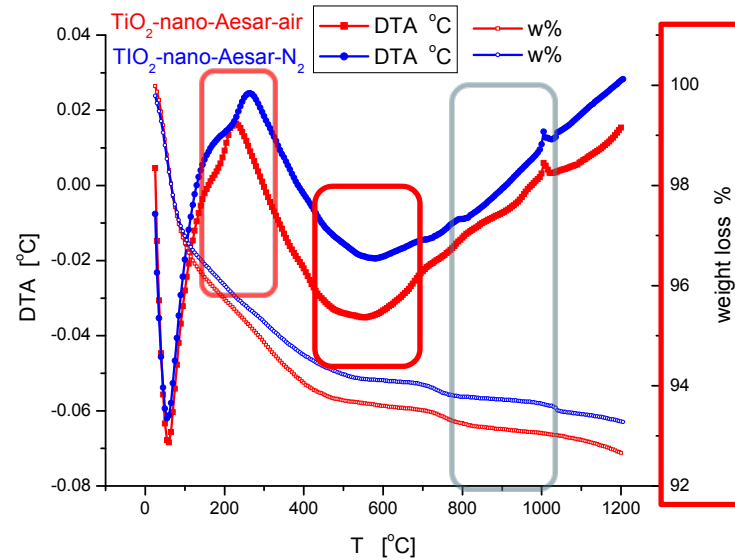
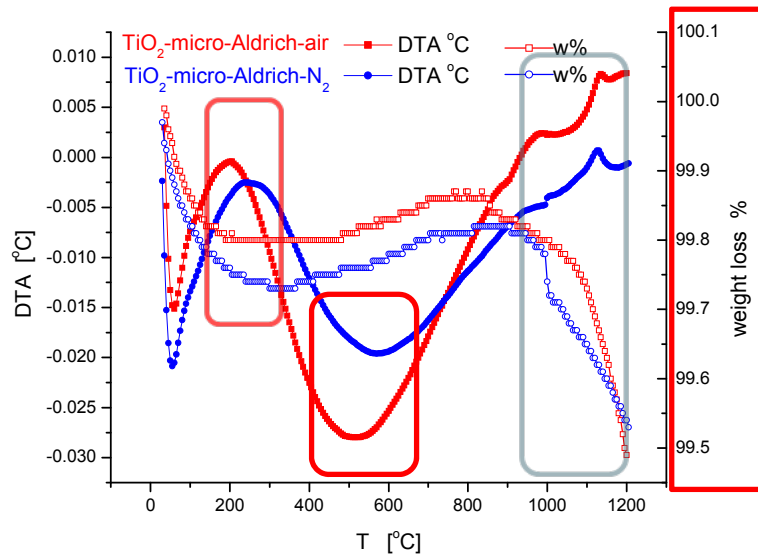
doi: 10.2298/SOS1403365L

UDK 549.514; 622.785

Influence of Nitrogen and Air Atmosphere During Thermal Treatment on Micro and Nano Sized Powders and Sintered TiO₂ Specimens

N. Labus^{1*}, S. Mentus^{2,3}, Z. Z. Đurić¹, M. V. Nikolić⁴

TiO₂ nano powder TiO₂ micro powder TG/DTA



Science of Sintering, **46** (2014) 365-375

doi: 10.2298/SOS1403365L

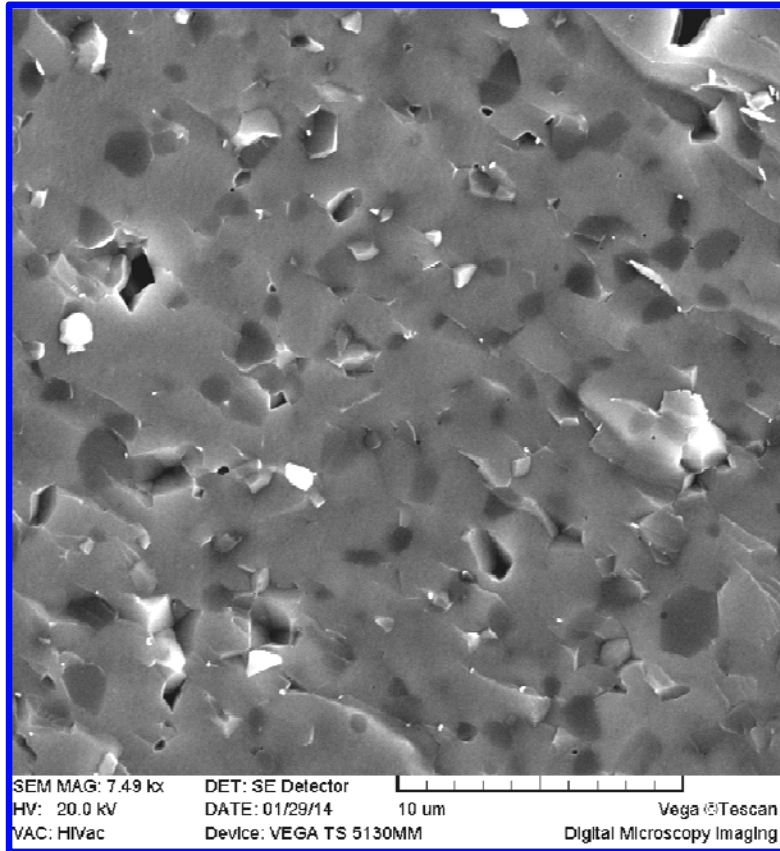
UDK 549.514; 622.785

Influence of Nitrogen and Air Atmosphere During Thermal Treatment on Micro and Nano Sized Powders and Sintered TiO₂ Specimens

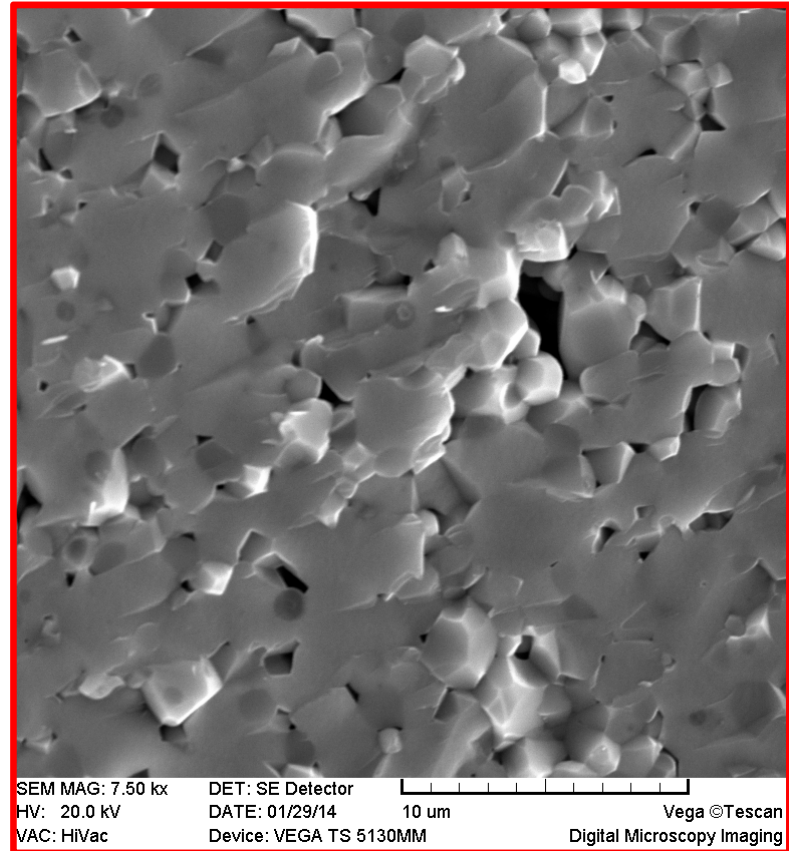
N. Labus^{1*}, S. Mentus^{2,3}, Z. Z. Đurić¹, M. V. Nikolić⁴

SEM TiO₂ sintered - reheated

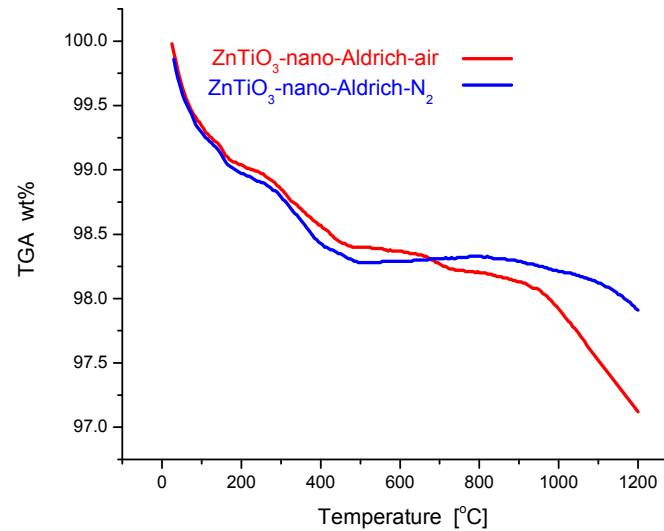
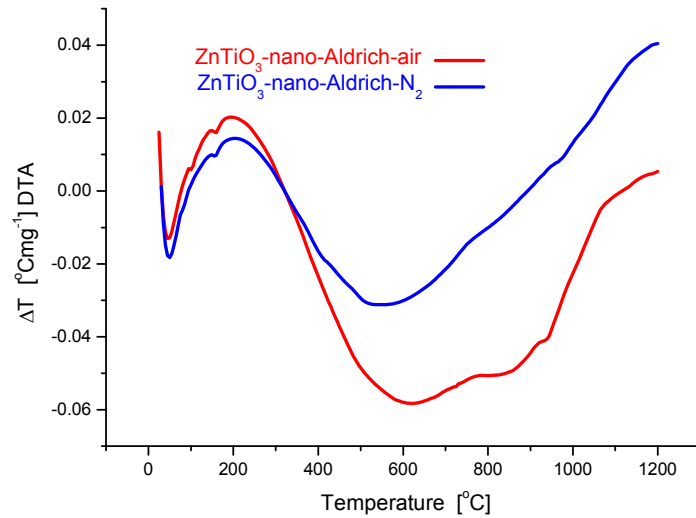
Nitrogen



Air



ZnTiO₃ nano powder TG/DTA



Science of Sintering, 47 (2015) 71-81

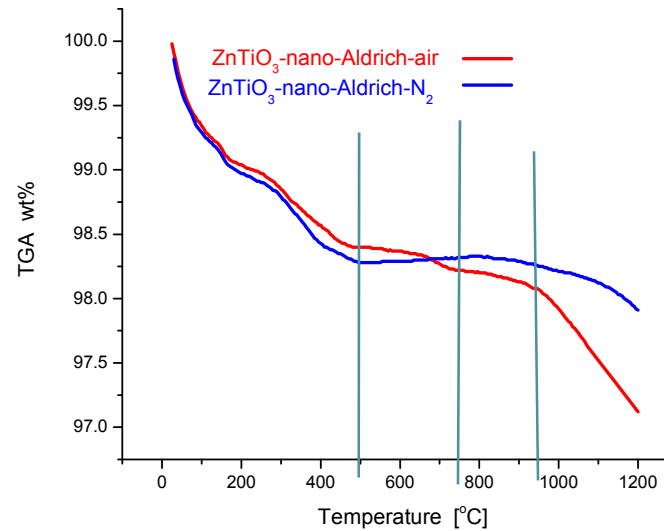
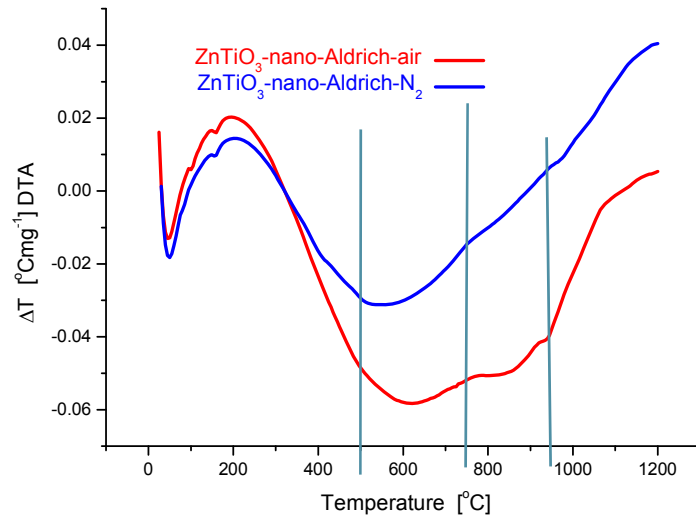
doi: 10.2298/SOS1501071L

UDK 622.785; 546.824

Reheating of Zinc-titanate Sintered Specimens

N. Labus^{1*)}, S. Mentus^{2,3}, S. Rakić⁴, Z. Z. Đurić¹, J. Vujačević¹, M.V. Nikolić⁵

ZnTiO₃ nano powder TG/DTA



Science of Sintering, 47 (2015) 71-81

doi: 10.2298/SOS1501071L

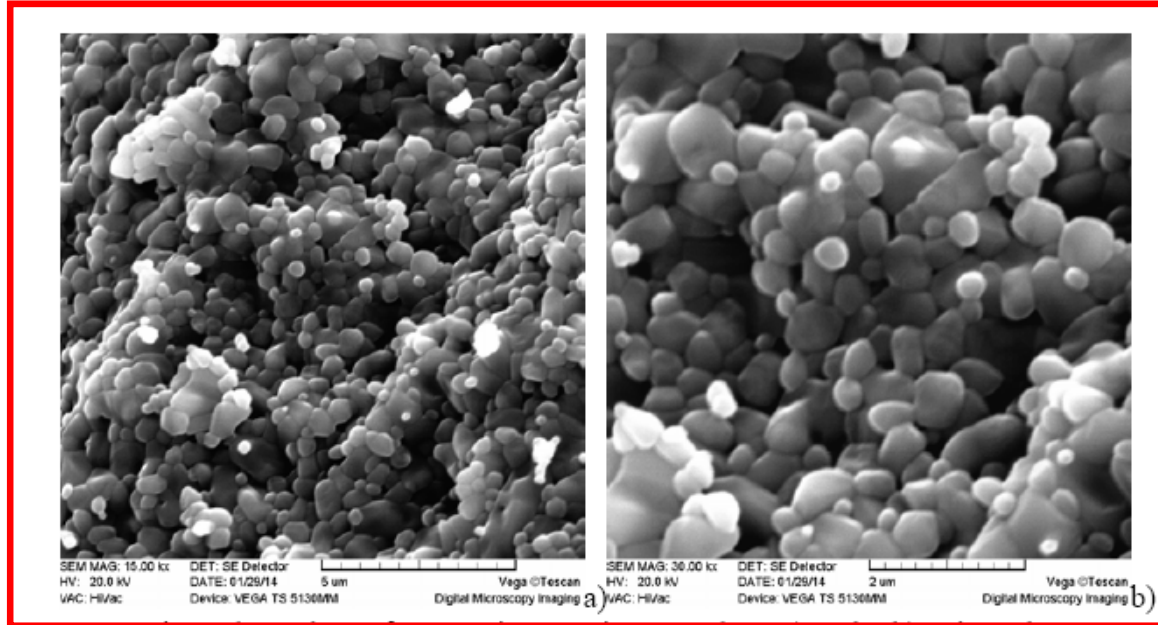
UDK 622.785; 546.824

Reheating of Zinc-titanate Sintered Specimens

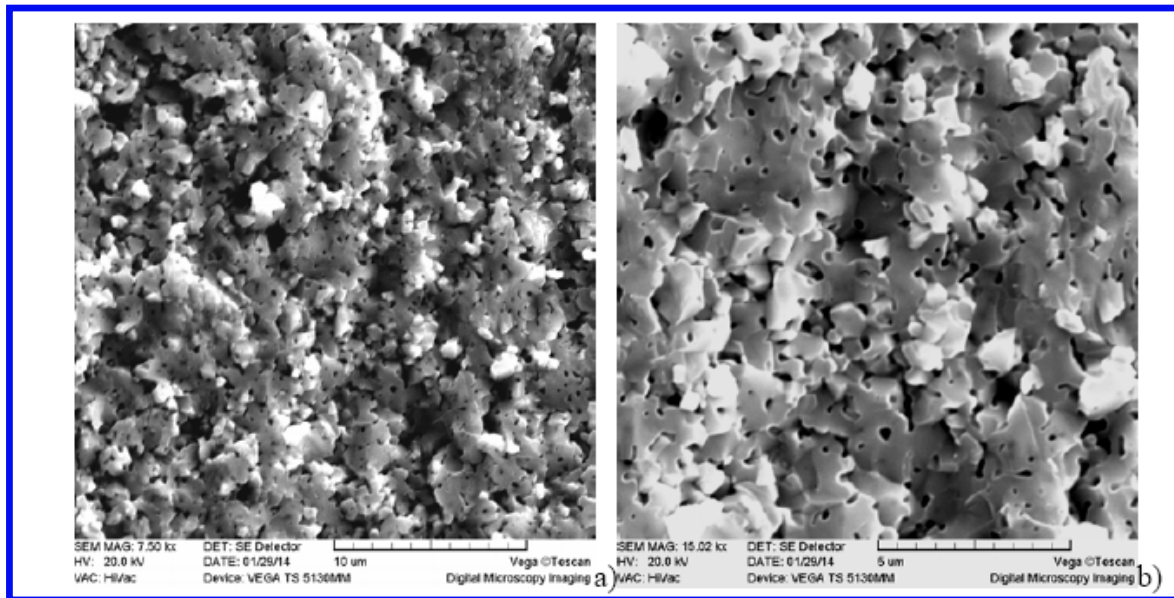
N. Labus^{1*)}, S. Mentus^{2,3}, S. Rakić⁴, Z. Z. Đurić¹, J. Vujačević¹, M.V. Nikolić⁵

SEM ZnTiO₃ sintered - reheated

Air



Nitrogen



CONCLUSION

- Oxides TiO_2 , ZnTiO_3 and $\text{Mn}_{1-x}\text{Zn}_x\text{Fe}_2\text{O}_4$ showed different dimension changes behavior during heating in air and nitrogen atmosphere.
- Microstructures observed on breakage showed completely different structure.
- Thermo gravimetric and differential thermal analysis showed that powder particle size plays fundamental role in atmosphere influence.